Proceedings of the 11th ICPMG 2026
11th International Conference on Physical Modelling in Geotechnics
8-12 June 2026, Zurich, Switzerland

Seismic performance of a 10 MW OWT on different foundation systems from dynamic centrifuge testing

C. Español-Espinel
Department of Engineering, University of Cambridge, UK, ce411@cam.ac.uk

D. Gaudio
Department of Structural and Geotechnical Engineering, Sapienza University of Rome, Rome, Italy, domenico.gaudio@uniroma1.it

S.P.G. Madabhushi
Department of Engineering, University of Cambridge, UK, mspg1@cam.ac.uk

ABSTRACT: As the offshore wind industry expands into the Asia-Pacific (APAC) countries, seismic considerations become important in the design of the foundations, especially when earthquake-induced liquefaction may occur. This paper presents centrifuge modelling of two foundations for offshore wind turbines (OWTs) installed in liquefiable soil, specifically a monopile, and an outrigger system, which aims to represent the behaviour of a jacket foundation. The performance of the two foundations in supporting identical OWTs subjected to a combination of operational and earthquake loading is discussed. The key findings suggest that the monopile experiences earthquake-induced rotation exceeding the allowable threshold recommended by DNV-ST-0126 and DNV-RP-0585. Although the outrigger exhibits less earthquake-induced rotation than the monopile, this advantage comes at the cost of larger settlements. Overall, the outrigger foundation provided a reasonably consistent solution for supporting OWTs in areas prone to liquefaction induced by earthquakes.

1 INTRODUCTION

Offshore wind technology had its early implementation in Northern Europe, where the monopile emerged as the preferred foundation system for Offshore Wind Turbines (OWTs) in shallow waters. Other regions in the world, including Japan and Taiwan, where there is a growing interest in deploying offshore wind energy, base their OWTs and foundation systems on European experiences. However, in these areas earthquakes pose challenges for current foundation systems such as monopiles and jackets, which were not originally conceived to withstand seismic loading and liquefaction. For this reason, several companies and institutions have launched ACE and ACE 2 (Alleviating Cyclone and Earthquake Challenges), two Joint Industry Projects (JIP) to make the design process for OWTs subjected to seismic loading more reliable. The first edition of this initiative resulted in the recommended practice for seismic design for wind power plants DNV-RP-0585 (2021), whereas ACE 2 aims at updating this standard by addressing specific topics such as damping and liquefaction. The guideline prescribes that foundation designs for OWTs in earthquake prone regions should be verified against the combined action of seismic and operational loading as one of the most important design load cases.

This scenario becomes critical when considering monopile-supported OWTs installed in soils susceptible to liquefaction, which may reduce the capacity of the soil to react to the loads transferred by the foundation, leading to significant rotation of the OWT. This problem has been recently studied by Español-Espinel *et al*. (2024), who conducted centrifuge modelling of a 7.11 m monopile subjected to combined operational and earthquake loading. The study revealed significant rotation of the monopile and superstructure that exceeded by far the allowable threshold of 0.5° set by DNV regulations. The capacity of the monopile was recently evaluated with 3D Finite Element analyses (Gaudio *et al*., 2025).

2 TEST DESIGN AND METHODOLOGY

This research compares the response of two different foundation systems for OWTs against combined static lateral and earthquake loading using centrifuge testing. In the first experiment, a monopile foundation was tested (Fig. 1a). Espanol-Espinel *et al*. (2025) developed the outrigger foundation, which was tested in the second experiment (Fig. 1b). The outrigger foundation incorporated a four-legged cruciform configuration with a skirted footing at the end of each leg. Both the monopile and outrigger were tested at a centrifuge acceleration of 70*g*.

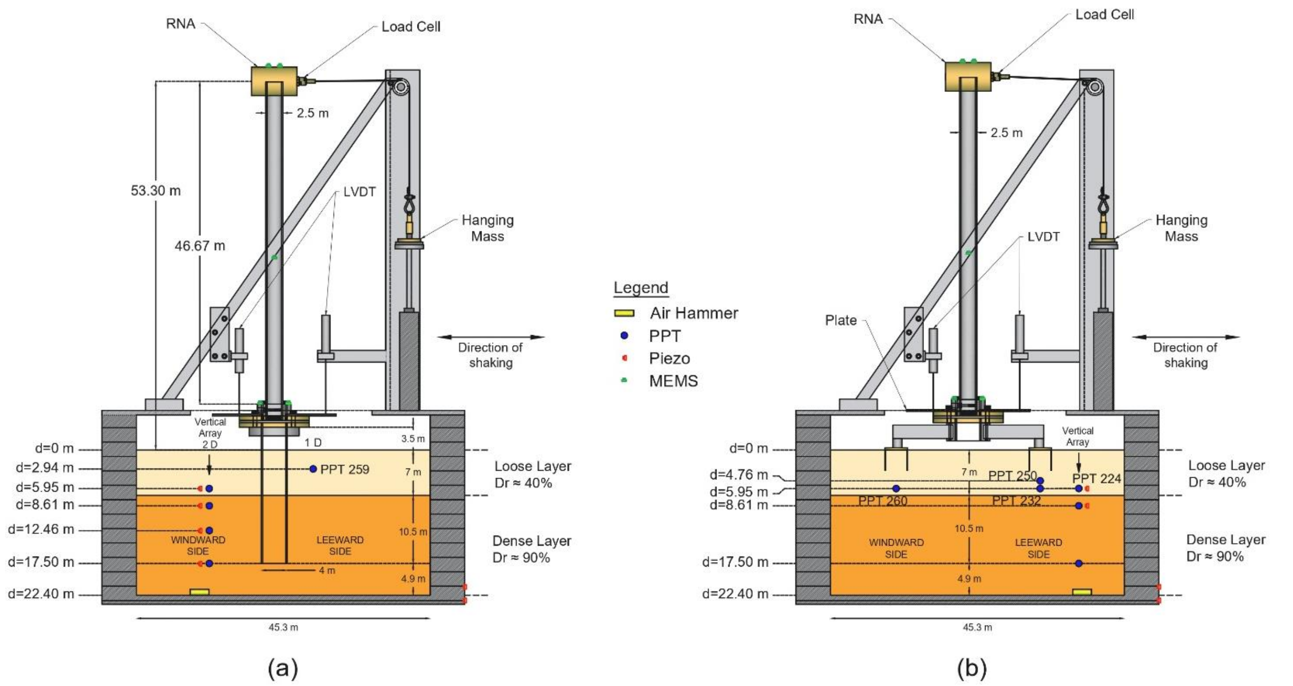

Figure 1. Problem layout at prototype scale: (a) Monopile-supported OWT; (b) outrigger system, (note: LVDT = linear variable differential transformer; PPT = pore pressure transducer; Piezo = piezo-accelerometer; MEMS = micro electromechanical system) (modified after Español-Espinel et al., 2025).

2.1 Experimental setup

The soil profile selected for testing of the two foundation systems included a 7-m-thick loose sand layer with $D_R \approx 40\%$, overlying a 15.4 m dense sand layer with $D_R \approx 85\%$. The sand sample was pluviated inside the ESB (Equivalent Shear Beam) model container using the automatic sand pourer at the University of Cambridge (Madabhushi *et al*., 2006). The ESB box (Brennan *et al*., 2006) is designed as a deck of rectangular aluminium frames interbedded with rubber sheets which increase in thickness towards the top of the container. Gaudio *et al*. (2023) suggested that the boundary effects of the ESB box in dynamic centrifuge testing result in less than a 20% deviation of the measured model response compared to free-field boundary conditions. Sand pouring was followed by full saturation of the loose and dense sand layers using the Cam-Sat System (Stringer and Madabhushi, 2009). The viscosity of the saturation fluid was augmented by a factor of 70, which is the scaling factor of the experiment, to satisfy the scaling laws for velocity and time in dynamic events (Madabhushi, 2014). After completing the preparation of the soil sample, the monopile and the outrigger system were installed at 1*g*. The operational moment at the mudline due to wind and waves was simulated using a loading rig comprising a base plate and a vertically mounted U channel that supports a pulley. The static lateral load was applied using hanging mass which was connected to the RNA by means of a steel wire that rests on the pulley. During the swing up process, the hanging mass was supported by a piston placed inside the U channel. Once the desired centrifuge acceleration was reached, the piston was retracted to release the hanging mass and apply the lateral load at the RNA. The hanging mass provided a static lateral load of 0.367 MN, which generated a moment of 20 MNm at ground level. The vertical load contributed by the RNA, tower, and transition piece is presented as V_{OWT} in Table 1.

2.2 Properties of the Foundations

As shown in Fig. 1, the diameter (D) and length of the monopile (L) tested was 4 m and 17.5 m respectively, whereas the height of the Rotor-Nacelle Assembly (h_{RNA}) from ground level was 53.30 m. Despite these dimensions being 2.25 times smaller than those of full-scale structures in the field, the aspect (L/D) and the eccentricity (h_{RNA}/D) ratios are comparable to those of real structure values (Tab. 1). Therefore, to replicate the behaviour that real monopile supported OWTs would exhibit against static lateral loading, the static moment at ground level was also scaled down by a factor of 2.25.

Distance scales times the scaling factor, whereas moment scales with the scaling factor to the cube as per the centrifuge scaling laws (Madabhushi, 2014).

The outrigger is a cruciform-shaped structure with four 9.1 m-long legs that extend from the base of the OWT at an angle of 15° on either side of the shaking axis (Fig. 2). The ends of the legs rest on 3.15 m diameter skirted footings that are driven to a depth of 3.5 m into the loose sand.

2.3 Loading Sequence

The two identical turbines supported respectively by the monopile and the outrigger, were subjected to the loading sequence summarised in Table 2. The static lateral loading was exerted using the loading rig, while the earthquakes were reproduced by means of a servo-hydraulic earthquake actuator that seated on one end of the beam centrifuge (Madabhushi *et al*., 2015).The actuator has a sufficiently broad frequency bandwidth to accurately reproduce the prototype frequencies required for earthquakes EQ1 and EQ2 at model scale. EQ1 consisted of a sine sweep which shook the OWT tower with a broad spectrum of frequencies at a very low Peak Ground Acceleration (*PGA*). This motion facilitates identifying the excitation frequencies of the superstructure. Following this, the tower was loaded laterally so that the OWT was subjected to combined static and dynamic loading during the second earthquake (EQ2), which was a sinusoidal wave. Such a signal is not intended to represent a realistic earthquake record, but rather to generate sufficient excess pore water pressure within the soil to trigger liquefaction. This 1 Hz signal, lasting ten cycles (Table 2), was intentionally used to clearly identify the effects of earthquake cycles on soil behaviour and the dynamic response of the OWT.

Table 1. Comparison of properties between the prototype monopile supported OWT and the DTU 10MW reference OWT (Shaofeng et al., 2021)

Properties	Prototype structure	Real structure
D (m)	4	9
L (m)	17.5	42.6
h_{RNA} (m)	53.30	149
L/D	4.38	4.73
h_{RNA}/D	13.33	16.56
F_H **at RNA** (MN)	0.367	1.5
M_{static} **at g.l.** (MNm)	20	278
V_{OWT} (MN)	14.83	17.81

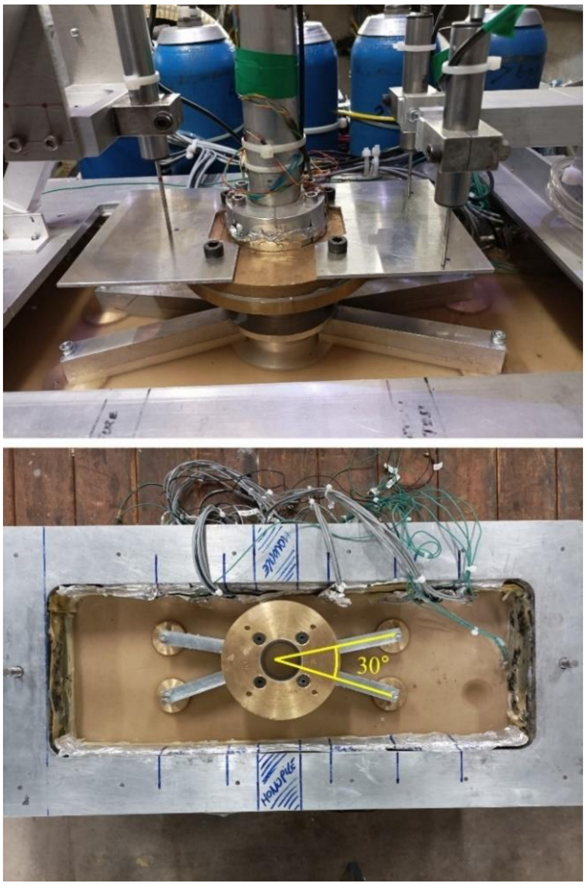

Figure 2. Side (top) and top view (bottom) of the outrigger (modified after Español-Espinel et al., 2025).

3 FOUNDATION PERFORMANCE UNDER SOIL LIQUEFACTION

This section addresses the dynamic response of the OWT. In addition, the performance of the monopile and the outrigger in the liquefiable soils is explored and compared.

3.1 Dynamic Response of the Superstructure

Although the prototype OWT is only one-third the height of a full-scale tower (Fig. 1), the bending stiffness and RNA mass of the model were adjusted to match the natural frequency (f_n) of a DTU 10 MW reference OWT. Alkhoury *et al*. (2020) predicted the first and second bending modes of excitation at 0.20 Hz and 1.44 Hz respectively. Fig 3 illustrates the frequencies at which the prototype OWT experiences excitation upon the application of the sine sweep (EQ1) for the two foundation scenarios here proposed. The first natural frequency of the prototype was encountered at 0.20 Hz, which corresponds to the value predicted by Alkhoury *et al*. (2020) for a DTU 10 MW turbine. However, no response is exhibited at the second mode of excitation.

3.2 Settlement and Rotation

As summarised in Section 2.3, earthquake EQ2 fired in this series of experiments was intended to liquefy the soil. The vertical array of sensors located in the far-field (Fig. 1) detected enough accumulation of excess pore water pressure, triggering liquefaction indeed (Fig. 4).

Soil liquefaction, combined with the static lateral moment provided by the hanging mass and the dynamic moment from the RNA mass itself, resulted in a large rotation of the OWT (Fig. 5). However, a significant variation in the amount of rotation was observed, depending on the foundation adopted. In the case of the monopile, most of the rotation took place during earthquake EQ2, although the structure slightly rotated after the earthquake until reaching almost 2.85°. By contrast, earthquake-induced rotation was reduced to 0.3° when the OWT was founded on the outrigger system. Following EQ2, the rotation increased progressively to 0.5°, which corresponds to the threshold allowed by DNV-ST-0126 (2021) and DNV-RP-0585 (2021). Nevertheless, the OWT experienced higher settlement when supported by the outrigger, which was not embedded up to the dense sand layer (Fig. 5). In the 80 seconds following the earthquake, the OWT with the outrigger foundation settled by an additional 97 mm, reaching a total settlement of 462 mm, compared with the monopile, which settled an additional 34 mm for a total of 319 mm. Such differences in the performance of the two foundation systems may be attributed to the mechanisms through which each foundation transfers the self-weight of the superstructure, the operational loads, and the inertial dynamic loading to the soil deposit. The sign and magnitude of excess pore pressure around each foundation indicate the stress distribution during and after the earthquake. In the case of the monopile, PPT-259 (Fig. 1a, depth d = 2.94 m within the loose sand layer) recorded negative excess pore pressure with values of approximately -20 kPa, towards the 8th cycle of EQ2, which indicates a tendency for soil dilation. Evidence of negative excess pore pressure below the outrigger foundation is provided in Fig. 6,

Table 2. Loading sequence applied to the OWT and foundations, including the monopile and outrigger.

M_{static} at g.l. (MNm)	Earthq.	*PGA* (*g*)	Frequency (Hz)	Cycles (-)
0	EQ1 (sweep)	0.03	0-5	-
Loading	-	-	-	-
20	EQ2 (wave)	0.18	1	10

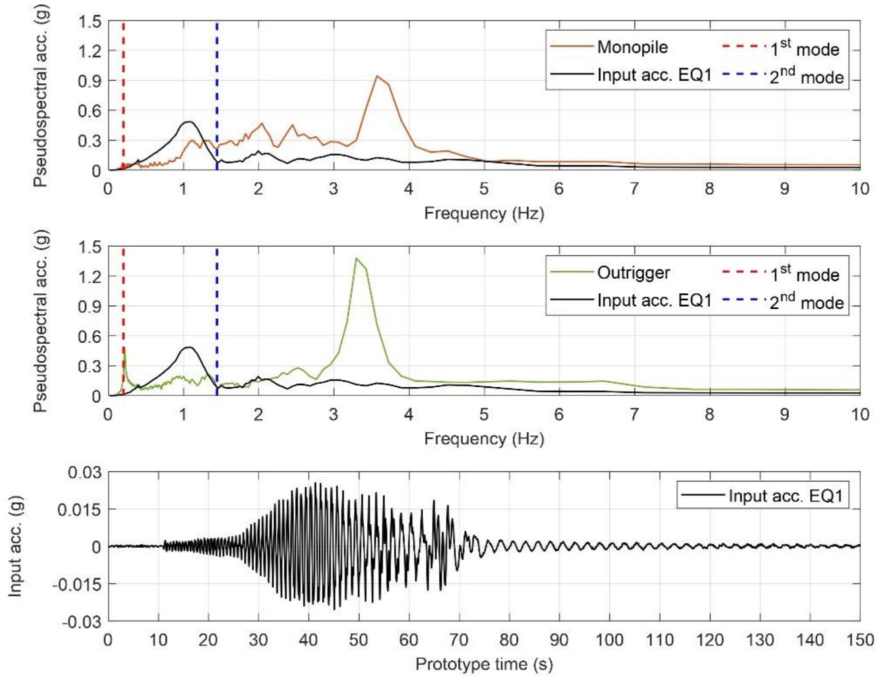

Figure 3. Pseudospectral accelerations derived from the RNA and input acceleration records for the OWT supported by monopile and outrigger foundation configurations. The first and second excitation modes of a DTU 10MW OWT, as calculated by Alkhoury et al. (2020), are superimposed. The input acceleration of EQ1 is depicted at the bottom (modified after Español-Espinel et al., 2025).

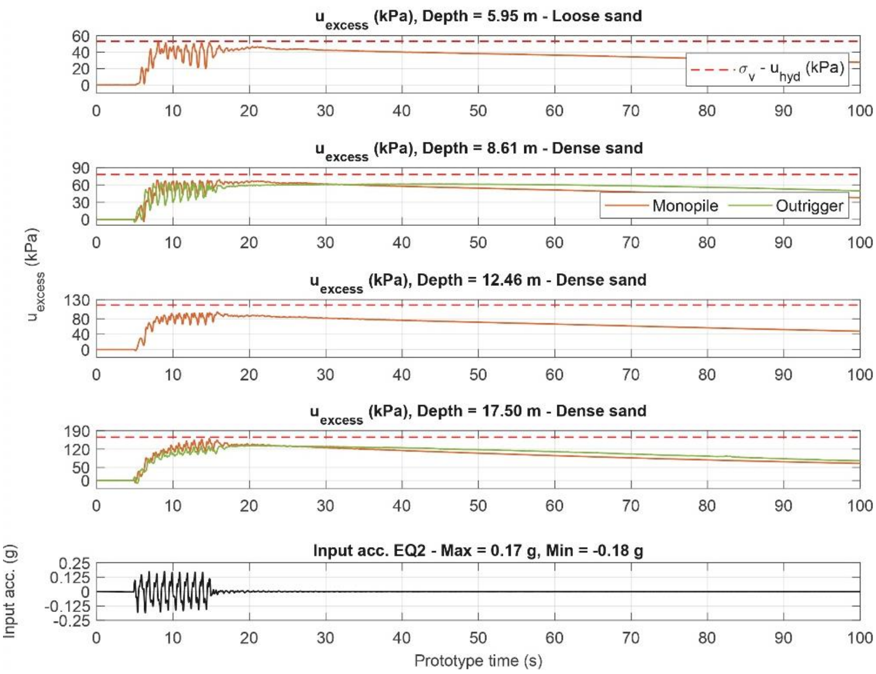

Figure 4. Excess pore water pressure recorded across the vertical array of sensors located in the far field (modified after Español-Espinel et al., 2025).

showing negative excess pore pressure of -12 kPa (PPT-260) and -55 kPa (PPT-232) below the windward and leeward skirted footings, respectively (Fig. 1b, depth $d = 5.95$ m within the loose sand layer). Moreover, the excess pore pressure measured in the far-field, 4.2 m away from the leeward skirted footing, rises to positive values exceeding 40 kPa, while the excess pore pressure below the skirted footings remains mostly negative in the period following the earthquake.

3.3 Earthquake-induced Moment

The magnitude of the dynamic moment is larger than that of the static moment and may have a greater impact on the overall rotation of the structure (Fig. 7). In the case of the monopile foundation, the dynamic moment is greater than that acting on the outrigger (Fig. 7). This increase is probably due to the tip of the monopile being located at a greater depth, where the denser sand and higher confinement state prevent the sand from fully liquefying. As a result, shear waves are capable of propagating through the denser soil and the monopile. The outrigger, conversely, is embedded in a loose sand layer that fully liquefies during the earthquake, except beneath the skirted foundations. The liquefied layer tends to filter the earthquake-induced shear stress generated by earthquake shaking, thus reducing the dynamic moment driving the rotation.

4 DISCUSSION

Two different foundation systems for OWTs, such as a monopile and an outrigger, were tested using dynamic centrifuge modelling at 70*g*. Both foundations withstood the self-weight of the OWT, the static moment generated by the operational load, and dynamic moment.

The findings of this research revealed significant differences in the performance of the two foundation types in terms of rotation and average settlement. As observed in Fig. 5, the monopile rotated 2.50° during the earthquake and up to 2.85° within the 80 seconds that followed the earthquake. In contrast, the outrigger experienced 0.30° that increased to 0.50° in the same timescales, due to post-earthquake consolidation effects. The disparity in rotation and

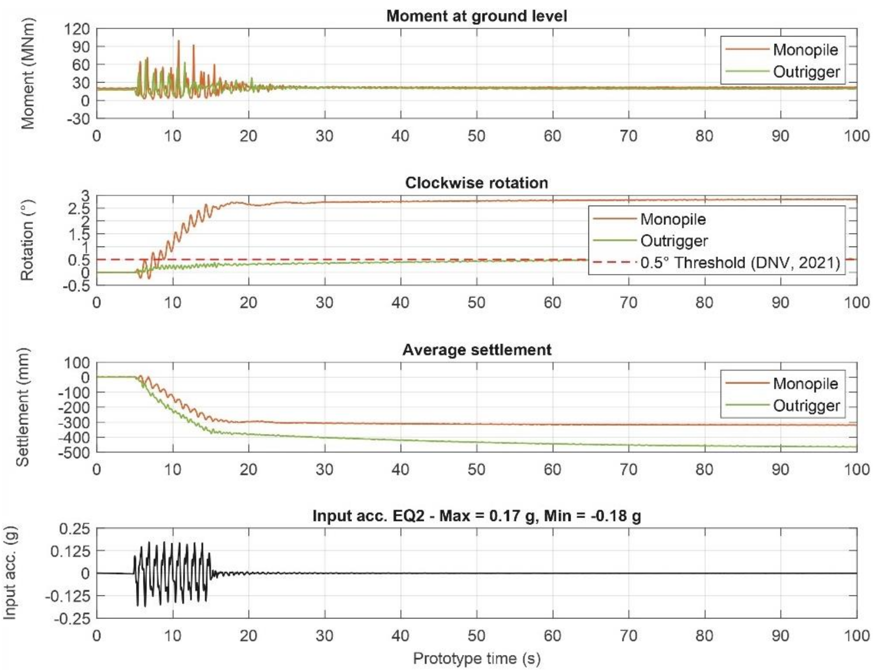

Figure 5. Time histories of moment at ground level (top), rotation and settlement (middle) experienced by the foundation systems considered in the study. The input motion of EQ2 is also shown at the bottom (modified after Español-Espinel et al., 2025).

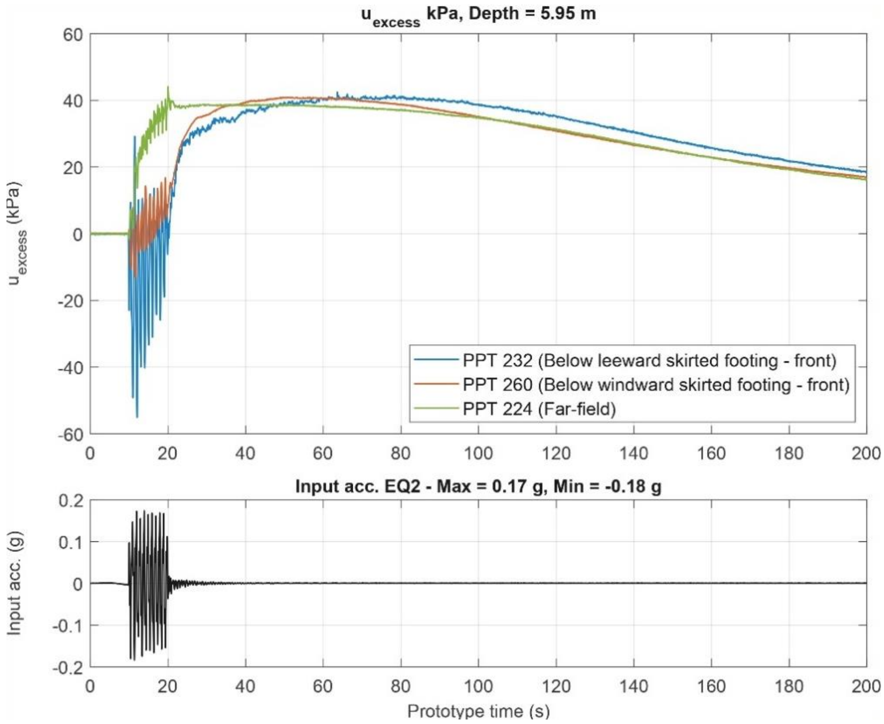

Figure 6. Excess pore water pressure recorded below the windward (PPT-260) and leeward (PPT-232) skirted footings of the outrigger, as well as at the far field (PPT-224), at a depth of d = 5.95 m. The input motion of EQ2 is also displayed at the bottom (modified after Español-Espinel et al., 2025).

settlement experienced by the OWT in each case depends on the mechanisms through which each foundation system transfers the loads from the superstructure onto the soil. First, the monopile supports the self-weight of the superstructure above it through skin friction. In addition, the static and dynamic moment resulting from operational and earthquake loading, respectively, are withstood by the lateral reaction of the soil against the monopile.

Static moment due to wind and waves translates into additional horizontal stress applied to the soil adjacent to the leeward side of the monopile. In this region, negative excess pore pressures were recorded, meaning that soil tends to dilate. However, the soil did not provide enough reaction force to counteract the stress applied by the monopile, resulting in substantial rotation of the OWT (Español-Espinel *et al*., 2025).The outrigger supported OWT experienced significantly less rotation, but larger settlements than the monopile. In this case, the stresses generated by the static and dynamic moments, as well as those caused by the self-weight of the OWT, were transferred directly to the soil through the footings.

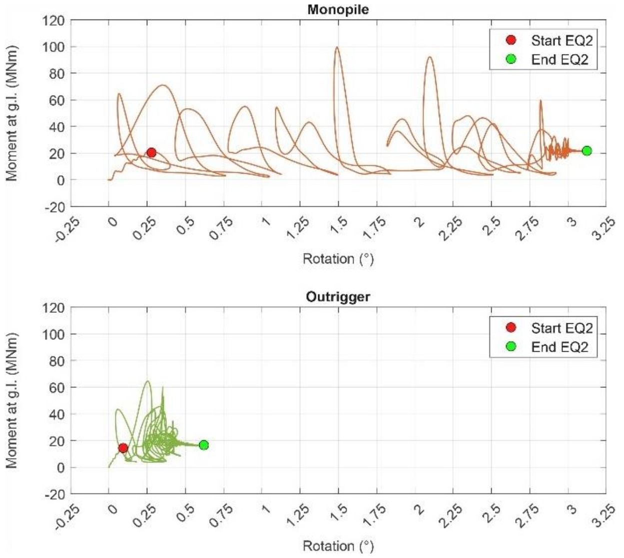

Figure 7. Moment-rotation response of the monopile and outrigger foundations induced by EQ2 (modified after Español-Espinel et al., 2025).

The negative excess pore pressure bulbs generated below the individual skirted footings of the outrigger were not large enough to prevent settlement of the foundation into the liquefied ground below. While this study focuses on a specific soil layering and relative densities, an increase in the relative density of the loose sand layer would significantly delay the onset of liquefaction. Similarly, a decrease in the thickness of the loose sand layer would result in additional soil stiffness provided by the thicker dense sand layer at the time of the earthquake. Thus, both monopile- and outrigger-supported offshore wind turbines would experience reduced settlement and rotation.

5 CONCLUSIONS

In this paper, the focus is on an alternative OWT foundation system to monopiles, aiming for improved performance under seismic loading, particularly in sands prone to liquefaction. Two types of foundations were investigated with the primary aim of increasing rotational stability of the OWT under the combined action of operational environmental load and seismic load as recommended by DNV-RP-0585 (2021).

The findings of this research suggest that commonly adopted monopile foundations may not be the most effective solution to support OWTs in seismic areas at risk of liquefaction. This study proposes an outrigger foundation to support OWTs in liquefiable soils, based on the principle that full liquefaction of the soil may be avoided if a sufficiently large stress is transferred to the soil.

The proposed foundation is an outrigger that includes four legs with skirted footings at their ends. Overall, the outrigger design exhibits reduced rotation compared to the monopile, although at the cost of higher settlements. While the monopile reached the underlying dense sand, the outrigger footings were embedded only within the loose sand layer, which is more prone to liquefaction. Such comparison may therefore be asymmetric, as settlement performance would likely improve significantly if the outrigger skirts reached the dense stratum.

Design guidelines such as DNV-ST-0126 (2021) and DNV-RP-0585 (2021) do not specify a clear threshold for maximum allowable settlement; however, they impose strict limits on foundation rotation, often limited to 0.5°. Serviceability considerations would typically govern the design rather than ultimate stability. In practice, this means that the allowable rotation limit could be exceeded within the first few cycles of an earthquake, even though the foundation capacity itself may not be reached.

ACKNOWLEDGEMENTS

The centrifuge experiments were performed with the excellent help of technicians at the Schofield Centre of University of Cambridge. This support is gratefully acknowledged. The second Author is also grateful for the financial support provided by Ministero dell'Università e della Ricerca (Italy) through the project PON "Ricerca e Innovazione" 2014-2020.

REFERENCES

Alkhoury, P., Soubra, A.H., Rey, V. and Aït-Ahmed, M. (2020). Natural frequencies estimation of a monopile supported DTU-10 MW Offshore Wind Turbine. *4th International Symposium on Frontiers in Offshore Geotechnics ISFOG - Austin, Texas.*

Brennan, A.J., Madabhushi, S.P.G. and Houghton, N. E. (2006). Comparing laminar and equivalent shear beam (ESB) containers for dynamic centrifuge modelling. *Proc 6th Int Conf Phys Mod Geotech, ICPMG 2006*. Leiden: Taylor and Francis, pp. 171-176.

DNV-ST-0126 (2021). Support structures for wind turbines. Standard DNV-ST-0126.

DNV-RP-0585 (2021). Seismic design of wind power plants recommended practice.

Español-Espinel, C., Haigh, S. K., Madabhushi, S. P. G., Abadie, C. N., Go, J. E. and Morrison, P. R. J. (2024). Evolution of excess pore water pressures around monopiles subjected to moderate seismic loading. *Soil Dyn Earthq Eng*, Vol. 176, 108316. DOI: https://doi.org/10.1016/j.soildyn.2023.108316

Español-Espinel, C., Gaudio, D. and Madabhushi, S.P.G. (2025). Investigating alternative foundation systems for offshore wind turbines in liquefiable soils. *Géotechnique*, Vol. 75, No. 10, pp. 1254-1268. DOI: https://doi.org/10.1680/jgeot.24.01059

Gaudio, D., Español-Espinel, C., Madabhushi, S.P.G. (2025). Vertical and Lateral Capacity of a Monopile in Layered Soils Using 3D Finite Element Analyses. In: Huynh, D.V.K., Doan, H., Cao, T.M., Watson, P. (eds) *Proceedings of the 3rd Vietnam Symposium on Advances in Offshore Engineering. VSOE 2024. Lecture Notes in Civil Engineering*, Vol 590. Springer, Singapore. https://doi.org/10.1007/978-981-96-3912-0_46

Gaudio, D., Seong, J., Haigh, S.K., Viggiani, G.M.B., Madabhushi, S.P.G., Shrivatsava, R., Veluvolu, R. and Padhy, P. (2023). Boundary effects on dynamic centrifuge modelling of onshore wind turbines on liquefiable soils, *International Journal of Physical Modelling in Geotechnics*, ICE Publishing, Vol. 23, No. 1, 16-34, ISSN: 1346-213X. DOI: https://doi.org/10.1680/jphmg.21.00085

Madabhushi, S.P.G., Houghton, N. E. and Haigh, S.K. (2006). A new automatic sand pourer for model preparation at the University of Cambridge. *Proc 6th Int Conf Phys Mod Geotech, ICPMG 2006*. Leiden: Taylor and Francis, pp. 217-222.

Madabhushi, S.P.G. (2014). Centrifuge modelling for civil engineers. Boca Raton, FL, USA: CRC Press, Taylor & Francis Group

Madabhushi, S.P.G., Haigh, S.K., Houghton, N.E. and Gould, E. (2015). Development of a servo-hydraulic earthquake actuator for the Cambridge Turner beam centrifuge. *International Journal of Physical Modelling in Geotechnics*, Vol.12, No. 2, pp. 77-88, DOI: https://doi.org/10.1680/ijpmg.11.00013

Natarajan, K. and Madabhushi, S.P.G. (2022). Seismic response of an offshore wind turbine jacket structure with pile foundations. *Soil Dynamics and Earthquake Engineering*, Vol.162, 107427.

Shaofeng, W., Torben-Juul, L., Bredmose, H. (2021). Ultimate load analysis of a 10 MW offshore monopile wind turbine incorporating fully nonlinear irregular wave kinematics. *Marine Structures*, Vol.76:102922.

Stringer, M.E. and Madabhushi, S.P.G. (2009). Novel computer-controlled saturation of dynamic centrifuge models using high viscosity fluids. *Geotechnical Testing Journal*, Vol.32, No. 6, pp. 559-564.